



Calhoun: The NPS Institutional Archive
DSpace Repository

NPS Scholarship

Theses

1971-09

Statistical results concerning the radiometric temperature changes sensed by NIMBUS II MRIR in the vicinity of the subtropical jet.

Knostman, Paul Brayton

Monterey, California ; Naval Postgraduate School

<https://hdl.handle.net/10945/15912>

This publication is a work of the U.S. Government as defined in Title 17, United States Code, Section 101. Copyright protection is not available for this work in the United States.

Downloaded from NPS Archive: Calhoun



Calhoun is the Naval Postgraduate School's public access digital repository for research materials and institutional publications created by the NPS community. Calhoun is named for Professor of Mathematics Guy K. Calhoun, NPS's first appointed -- and published -- scholarly author.

Dudley Knox Library / Naval Postgraduate School
411 Dyer Road / 1 University Circle
Monterey, California USA 93943

<http://www.nps.edu/library>

STATISTICAL RESULTS CONCERNING
THE RADIOMETRIC TEMPERATURE
CHANGES SENSED BY NIMBUS II MRIR
IN THE VICINITY OF THE
SUBTROPICAL JET

PAUL BRAYTON KNOSTMAN

LIBRARY
NAVAL POSTGRADUATE SCHOOL
MONTEREY, CALIF. 93940

LIBRARY
NAVAL POSTGRADUATE SCHOOL
MONTEREY, CALIF. 93940

United States Naval Postgraduate School



LIBRARY
NAVAL POSTGRADUATE SCHOOL
MONTEREY, CALIF. 93940

THESIS

STATISTICAL RESULTS CONCERNING THE RADIOMETRIC
TEMPERATURE CHANGES SENSED BY NIMBUS II MRIR
IN THE VICINITY OF THE SUBTROPICAL JET

by

Paul Brayton Knostman

Thesis Advisor:

F. L. Martin

September 1971

Approved for public release; distribution unlimited.

LIBRARY
NAVAL POSTGRADUATE SCHOOL
MONTEREY, CALIF. 93940

Statistical Results Concerning the Radiometric
Temperature Changes Sensed by NIMBUS II MRIR
in the Vicinity of the Subtropical Jet

by

Paul Brayton Knostman
Lieutenant Commander, United States Navy
B.A., Whitman College, 1961

Submitted in partial fulfillment of the
requirements for the degree of

MASTER OF SCIENCE IN METEOROLOGY

from the

NAVAL POSTGRADUATE SCHOOL
September 1971

ABSTRACT

Radiances obtained from the 11- μ window channel by MRIR scanning radiometer of NIMBUS II were investigated in order to determine areas of time change of T_2 , which may be related to effective cloud top level of the five-day mean cloud state. A statistical model was developed that is useful in obtaining a valid specification for effective cloud top change, using a stepwise regression program.

The parameters ΔT_1 , ΔZ , and \bar{T}_2 appear to provide the necessary spatial and temporal stability to employ the specification scheme over a time span of ten days. These three parameters are all highly descriptive of ΔT_2 in terms of basic atmospheric dynamical relationships. It is recommended that a test be made of this hypothesis using a 24-hour specification procedure.

TABLE OF CONTENTS

I.	INTRODUCTION -----	8
II.	PROCESSING OF DATA -----	11
III.	STATISTICAL PROCEDURES -----	14
	A. EXPERIMENTS FOR DETERMINING PREDICTION TIME-STEPS -----	14
	B. TEST FOR AN OPTIMAL NUMBER OF PREDICTORS -----	17
	C. REQUIREMENTS FOR A USEFUL SPECIFICATION FOR T_2 ---	20
	D. ASSESSMENT OF THE USEFULNESS OF THREE-PREDICTOR RELATIVE TO FOUR-PREDICTOR CASES -----	21
IV.	STATISTICAL RESULTS AND INTERPRETATION -----	23
	A. TABULAR LISTINGS OF THE INDIVIDUAL SPECIFICATIONS AND VERIFICATIONS -----	23
	B. A SUMMARY OF THE MEAN SPECIFICATION- PREDICTION RESULTS -----	30
	C. NORMAL PATTERNS OF PREDICTOR-ENTRY FOR USEFUL SPECIFICATION OF ΔT_2 -----	32
V.	EXTENSION OF THE RESULTS TO 24-HOUR SPECIFICATIONS ---	35
	A. RE-EXAMINATION OF THE FIVE-DAY SPECIFICATION PROCEDURE FOR POSSIBLE EXTENSION -----	35
	B. 24-HOUR STATISTICAL SPECIFICATION OF ΔT_2 AND THE PHYSICAL INTERPRETATION OF THE PREDICTOR VARIABLES -----	36
	1. The 24-Hour Time Change, ΔT_1 -----	37
	2. The 24-Hour Height Change at 500 mb, ΔZ -----	38
	3. The Large-Scale Steering Parameter, T_2 -----	39
VI.	PROPOSALS FOR FUTURE STUDY -----	42
	BIBLIOGRAPHY -----	44
	INITIAL DISTRIBUTION LIST -----	45
	FORM DD 1473 -----	46

LIST OF TABLES

TABLE		Page
1	The critical F_j^G statistics at the 95% confidence limit for entry of the Jth predictor set of P=4 variables -----	17
2	Specification of the predictors and their order of entry in equation (2) and for the map period corresponding to time k=1 -----	19
3	Specification of ΔT_2 by means of three predictors for time k=2 -----	23
4	Specification of ΔT_2 by means of three predictors for time k=3 -----	24
5	Specification of ΔT_2 by means of three predictors for time k=4 -----	24
6	Specification of ΔT_2 by means of three predictors for time k=5 -----	25
7	Specification of Δl_2 by means of three predictors for time k=6 -----	25
8	Specification of ΔT_2 by means of three predictors for time k=7 -----	26
9	Specification of ΔT_2 by means of three predictors for time k=8 -----	26
10	Specification of ΔT_2 by means of three predictors for time k=9 -----	27
11	Specification of ΔT_2 by means of three predictors for time k=10 -----	27
12	Specification of ΔT_2 by means of three predictors for time k=11 -----	28
13	Specification of ΔT_2 by means of three predictors for time k=12 -----	28
14	Specification of ΔT_2 by means of three predictors for time k=13 -----	29
15	Specification of ΔT_2 by means of three predictors for time k=14 -----	29

TABLE

Page

16	Summary of percentage explained variances of ΔT_2 at the specification step k , and at step $(k+1)$ in the verification process -----	31
17	The predictand-predictor linear correlation matrix for map 2 -----	33

LIST OF SYMBOLS

A_i	regression coefficients for ΔT_2 in a four-variable 5-day mean specification
B_i	regression coefficients for ΔT_2 in a three-variable 5-day mean specification
C_i	regression coefficients for ΔT_2 in a 24-hour specification
\bar{C}	mean cloud cover at grid point (i,j)
F_j	test ratio of mean squares
i	x-direction grid indicator
j	y-direction grid indicator
J	regression step indicator
k	time-step indicator
n	number of grid points in data sample
NESS	National Environmental Science Services
P	number of predictors among X_1, \dots, X_4 employed in regression
R	multiple correlation coefficient
$\sigma_{Y/X}$	standard error
σ	standard deviation
T	equivalent black body temperature at (i,j), sensed in channel 1 or 2
X	predictor in specification equation
Z	geopotential height at 500 mb

ACKNOWLEDGEMENT

The author gratefully acknowledges the enthusiastic encouragement and assistance offered by Professor Frank L. Martin during the research and writing of this thesis. The author's thanks also go to Professor Wm. van der Bijl for his constructive suggestions in the final preparation of the text.

I. INTRODUCTION

The diagnosis of weather features by sequential analysis of satellite maps of infrared radiances sensed during the lifetime of the NIMBUS II satellite, presents opportunities for understanding tropical and subtropical atmospheres generally, and in particular the environment of the subtropical jet stream. These radiances were obtained by the MRIR scanning radiometer of NIMBUS II, which scanned in the $11\text{-}\mu$ window channel (channel 2) and gave an equivalent blackbody temperature (hereafter called T_2). This radiometer also scanned in the $6.7\text{-}\mu$ water vapor channel (channel 1), which corresponds to the effective water-vapor temperature (hereafter called T_1) in the upper troposphere. For a more detailed discussion of MRIR data, the reader is referred to the NIMBUS II User's Guide (Staff, 1966).

Grid point maps of the two equivalent blackbody temperature fields T_1 and T_2 for the period 15 May through 28 July 1966 were provided in the form of five-day means through the kind auspices of the Laboratory for Atmospheric and Biological Sciences of NASA at Greenbelt, Maryland. The use of five-day mean maps presented consecutive fields with no data gaps on the quasi-globe defined between 70S - 70N latitude (Fig. 1), although all of the transient daily features have undoubtedly been smoothed out.

The purpose of this research was to specify statistically the time change of T_2 , denoted hereafter as ΔT_2 , especially in data-sparse areas over the oceans. The actual value of ΔT_2 may be related to the change in the effective or mean cloud-top level of the five-day mean cloud state at grid point (i,j) . In turn the field of $\Delta T_2(i,j)$ will be

statistically related to certain derived products which are descriptive of basic atmospheric processes.

Areas of significant ΔT_1 values are known to be related to areas of variation in the cirriform cloud-top level and/or variation in depth of moist layers associated with updrafts or downdrafts in the layer 6-10 km [Raschke and Bandeen (1967), Beran, et al. (1968)]. During the course of this investigation it became evident that ΔT_1 is a most descriptive parameter for specifying ΔT_2 , and hopefully is amenable to prognostication for periods up to 12 hours in advance of the latest radiometric swath. If so, the method described here could be altered to provide a 12-hour prediction for ΔT_2 .

Although radiometric data covered the region 70S-70N in Mercator grid coordinates, the area of interest for this study was restricted to the limits 14.3N to 56.8N for which area five-day 500 mb contour data were available. At the same time, these limits provided sufficient latitude to accommodate each of the subtropical jet streams considered. The longitude span of the subtropical jet area was restricted for the purposes of this study to the range 180W to 120W. This area could normally be classified as data-sparse. During the data period of this study, the area displayed well defined five-day mean subtropical jet coverage.

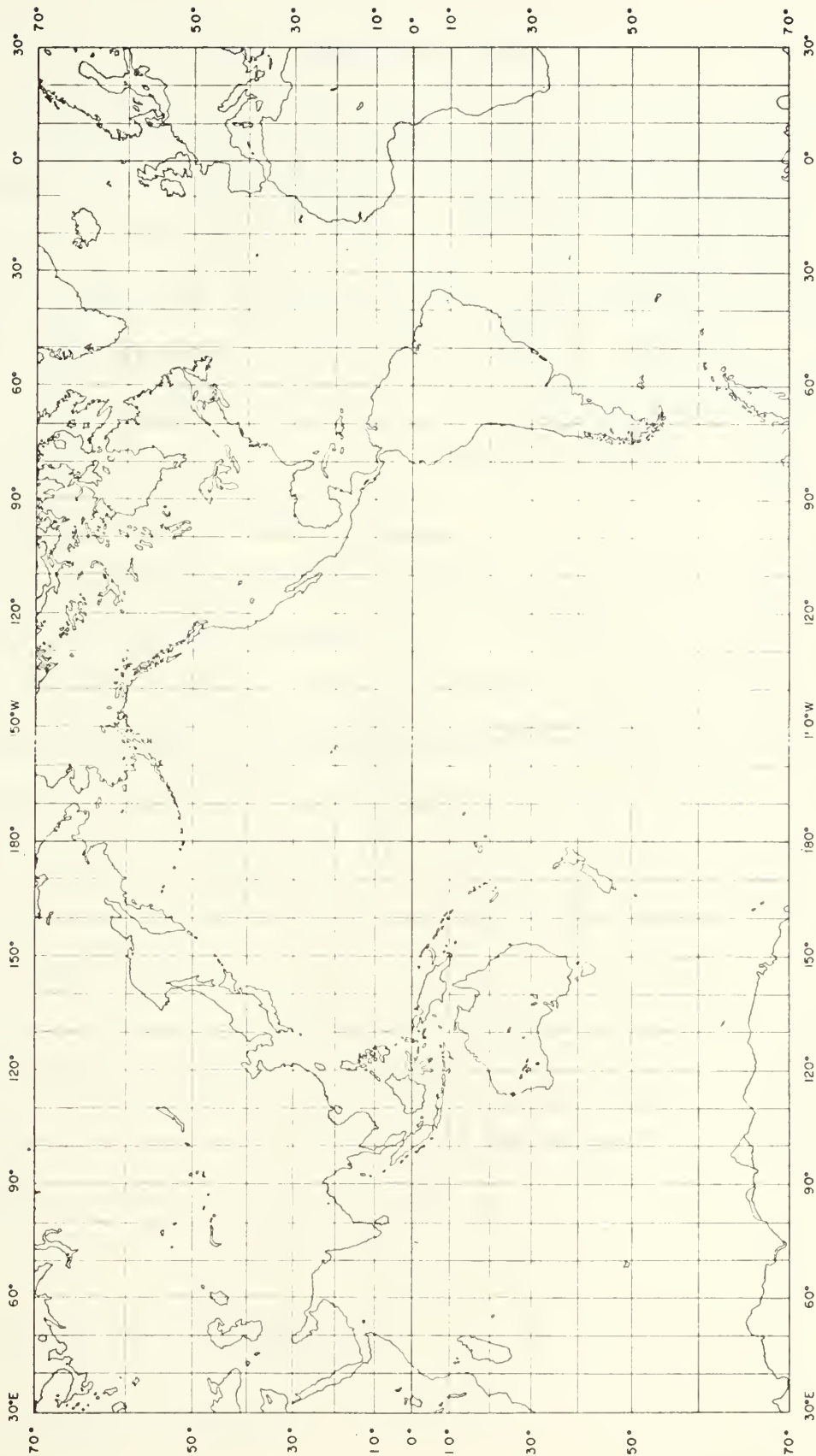


Fig. 1. Mercator grid point chart over which radiometric data were distributed.

II. PROCESSING OF DATA

The radiometric data were distributed over a Mercator grid point chart having $i=1, \dots, 73$ grid points in the longitudinal direction, and $j=1, \dots, 41$ rows of latitude covering the meridional span 70S-70N. The Mercator base chart had a superimposed square mesh grid, with a mesh interval d equivalent to five degrees of longitude, true at the equator (Fig. 1). The radiometric data $T(i,j)$ were subjected to an initial filtering which eliminated waves of two gridmesh lengths, but left unaffected all waves of length $L \geq 8d$.

As a possible dynamic predictor, the five-day mean 500 mb Northern Hemisphere non-overlapping contour fields for five-day map periods synoptic with the radiometric temperature fields were also obtained in punched card format covering the longitude dimension just described, but limited to 18 gridpoint rows poleward of latitude 14.3N (i.e., to 56.8N in Fig. 1). It should be noted that the contour map fields were sufficiently smooth that preliminary filtering was not considered necessary for these fields.

Certain operations are defined as representing the time-mean and time-differencing operations on temperature data at each grid point of the successive maps. These time centered operations are defined below:

Temperature-mean considered at time k :

$$2\bar{T}_k(i,j) = T_{k+1/2}(i,j) + T_{k-1/2}(i,j)$$

Temperature-time difference at k :

$$\Delta T_k(i,j) = T_{k+1/2}(i,j) - T_{k-1/2}(i,j)$$

where $T_{k+1/2}$ = radiometric five-day mean temperature centered at time $k+1/2$

i = x-direction grid indicator

j = y-direction grid indicator

$k = 1, 2, \dots, 14$, the time-step indicator (half steps are centered at times of individual five-day means, Fig. 2).

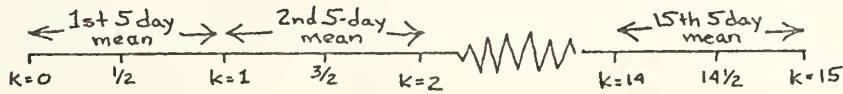


Fig. 2. Illustrating time-sequencing of five-day mean periods, and the time-index scheme used in centered time differencing.

A similar procedure was followed to form ΔZ by subtraction of successive five-day mean 500-mb contour fields which are also centered at the half time-steps indicated in Fig. 2.

A computer program was generated to carry out these time-centered computations over the meridional range 14.3°N - 56.8°N as well as over the longitudinal extent of this investigation. This resulted in a set of fourteen consecutive maps, each of which consisted of five fields of time-means and time-differences of the following parameters: $\Delta T_{1,k}$, $\bar{T}_{1,k}$, $\Delta T_{2,k}$, $\bar{T}_{2,k}$, ΔZ_k . These fields were programmed for production both in punched card and print-out forms.

Fifteen consecutive subtropical jets in the eastern Pacific were manually determined using the fifteen original five-day mean 500-mb contour maps for the periods centered at times $t=k+1/2$, with $k=0, \dots, 14$. The selection of individual jet-latitude coordinates was made by examining the test area 180°W - 120°W for the latitude of the tightest contour gradient that could be assigned nearest to the subtropical anticyclone on the five-day mean 500-mb chart.

These five-day mean subtropical jets lay well within the previously described latitude range of 14.3N-56.8N in which range most of the large contour-change ΔZ centers could be located. Furthermore the fifteen geostrophic mean jets varied only slightly in time and space, so that an average of six grid points lay both to the north and south sides of the jet. In order that the statistical test area be consistently more extensive than the jet area, the data set was expanded longitudinally to include two gridpoints west of 180W and three to the east of 120W. Thus the sample size for each of the $k=1, \dots, 14$ map-differenced times was constant at 216 in this investigation.

III. STATISTICAL PROCEDURES

A. EXPERIMENTS FOR DETERMINING PREDICTION TIME-STEPS

The Biomedical stepwise regression program, BMD02R [Dixon, 1966], was used in the statistical experiments described in the following pages. A brief summary of symbols and equations follows.

When the statistical specification is made for ΔT_2 , the predictors are understood to be X_1, X_2, X_3, X_4 , defined at mean map time k , and each grid-point (i,j) as:

$$\begin{aligned} X_1 &= (T_{1,k+1/2} - T_{1,k-1/2}) = \Delta T_{1,k} \\ X_2 &= (Z_{k+1/2} - Z_{k-1/2}) = \Delta Z_k \\ X_3 &= (T_{2,k+1/2} + T_{2,k-1/2}) = 2\bar{T}_{2,k} \\ X_4 &= (T_{1,k+1/2} + T_{1,k-1/2}) = 2\bar{T}_{1,k} \\ \Delta T_{2,k} &= (T_{2,k+1/2} - T_{2,k-1/2}) \end{aligned} \tag{1}$$

The variables defined in (1) appear in the sets of specification equations associated with $\Delta T_2(k)$ in the form

$$\Delta T_2 = A_0 + A_1 X_1 + A_2 X_2 + A_3 X_3 + A_4 X_4 \tag{2}$$

where A_i are the regression coefficients, selected in a stepwise manner by the program BMD02R.

In order to estimate the variable ΔT_2 centered at any one given map-time k from the concurrent predictor set in (1), it was necessary to determine how large a sample base of dependent data was needed. This question was tentatively answered by performing the following three

statistical experiments, each of which tested not only the significance of the specifications but also the stability of the regressions for at least one map-period.

1. Each of thirteen time-centered periods (i.e., at time $k=1,2,\dots,13$) was used to generate a specification equation (2) which could be used with the data of the next period (i.e., at times $k=2,3,\dots,14$) leading to a set of thirteen verifications. This experiment gave the best individual period specifications and also single-period verifications on the test used in the experiments described below. The order of entry of the predictors varied less from case to case, implying greater stability in this system of deriving the specification equations than in tests 2 or 3 described below.
2. The seven odd-numbered map-time fields were pooled in order to generate a single composite specification equation. The coefficients of this equation were used to operate on the variables X_1 , X_2 , X_3 , and X_4 of equation (2) at the even-numbered time periods, so that, in effect, a composite single-period forecast scheme was devised. In this case, the specification equation itself did not afford sufficient explained variance of the predictand ΔT_2 for a valid comparison with the results of tests 1 and 3. The transgenerated equation explained even less significance when applied to the composited seven-day test data (at times $k=2,4,\dots,14$). This method indicates the lack of statistically homogeneous samples when drawn from a meteorological period encompassing 13 five-day mean maps, or 65 days.
3. The final test undertaken was to use a pooled data base consisting of three consecutive periods (e.g., $k=1,2,3$) in order to generate a three-map

composite specification equation for use in predicting ΔT_2 for the single following period (e.g., $k=4$). This set of apparent single-step forecasts was verified against the known data for time $k=4$.

Similarly, the succeeding three-period pooled data base for times centered at $k=2,3,4$ was used for a composite statistical sample to provide a verification at map-time $k=5$, and likewise on to the final period $k=14$.

Test 3, which used a data base of pooled data from three consecutive maps in order to transgenerate an estimated ΔT_2 for the fourth in succession actually involved on the average a full two-period verification test. This test was simply not as effective in describing explained variance on the independent sample as test number 1 described above, which involved single-map time-steps. Hence all results to be considered in Tables 2 and following are based upon the results of test 1 only. As previously noted these comparative tests were primarily based upon the relative stability of the verification procedures carried out upon independent data.

The definitions X_1, X_2, X_3 and X_4 serve to simplify the description of the results in Table 2(a) below. This table refers to the order of entry of the four variables in the specification equation associated with ΔT_2 of equation (2).

The determination of the F-statistic upon entry, computed at each step of the multiple regression program (BMD02R), forms the basis for the order of entry of the variables X_i in Table 2.

The definition of the F-statistic at the Jth step of entry is defined as:

$$F_J[1, n-J-1] = \left\{ \frac{[\text{cum. \% exp. var., step } J] - [\text{cum. \% exp. var., } J-1]}{[\text{remaining \% var. after step } J]} \right\} \quad (3)$$

Here n is the number of grid points in the data sample. Since significance is sought at the 95% level of confidence for the J th variable added, F_J is compared with a critical value F_J^C suggested by Miller (1962) as

$$F_J^C = F_{\alpha/(P-J+1)}(1, n-J+1), \quad \alpha = .05$$

where P is the number of predictors among X_1, \dots, X_4 employed in the regression. The sequence of F_J^C values is easily deduced from tables of F-values at the indicated rejection limits for $\alpha/(P-J+1)$. These critical F_J^C -values are listed below for the J th selection step.

TABLE 1. The critical F_J^C statistics at the 95% confidence limit for entry of the J th predictor of a total predictor set $P=4$ variables. The sample size is $n=216$ in each case. The last row shows the corresponding critical values when only three predictors are considered for entry by the stepwise regression.

J \ P	J=1	J=2	J=3	J=4
P=4	6.34	5.83	5.12	3.89
P=3	5.83	5.12	3.89	

B. TEST FOR AN OPTIMAL NUMBER OF PREDICTORS

The stepwise regression technique applied to ΔT_2 and its predictor-set X_1, \dots, X_4 on map-day 1 led to the results shown in Table 2(a). Comparison of the F_J upon entry with the critical values in Table 1 at steps $J=1, \dots, 4$ indicates that the fourth predictor entering does so with a very low F-value and a resulting low probability of rejecting the null hypothesis that A_4 equals 0 in equation (2). However the first three predictors all entered with confidence levels in Table 2(a) well in excess of the 95% level of belief.

Part (b) of Table 2 contains the specification results for ΔT_2 at map-time 1 with the variable $2\bar{T}_1$ excluded from the predictor set by means of an option of the BMD02R program. The predictor set in Table 2(b) is now reduced to ΔT_1 , ΔZ and $2\bar{T}_2$. An objective rationale for the statistical preference of $2\bar{T}_2$ to $2\bar{T}_1$ is given in more detail in IV(C), p 32.

In Table 2(c), the stability of the specification equation at time $k=1$ is tested by correlating the observed ΔT_2 values of sample map 2 against the values estimated from the transgenerated equation for $\Delta T_2(k=2)$, made by using the day 1 coefficient matrix listed in Table 2(a). Symbolically this operation is performed using the estimator matrix equation:

$$\widehat{\Delta T}_2(2) = (A_0, A_1, A_2, A_3, A_4) \begin{pmatrix} 1 \\ X_1 \\ X_2 \\ X_3 \\ X_4 \end{pmatrix} \quad k=2 \quad (4)$$

Here coefficients A_i are determined from the program BMD02R and are listed in column 6 of Table 2(a).

Some question exists regarding the relative stability of the four-predictor equation (4) compared to the three-predictor equation inherently given in Table 2(b). This three-predictor transgenerated estimator is denoted by the symbol $\widetilde{\Delta T}_2(2)$ for day 2 and has the form:

$$\widetilde{\Delta T}_2(2) = (B_0, B_1, B_2, B_3, 0) \begin{pmatrix} 1 \\ X_1 \\ X_2 \\ X_3 \end{pmatrix} \quad k=2 \quad (5)$$

Here the B_i are the coefficients listed alongside the predictors in Table 2(b).

TABLE 2. Specification of the predictors and their order of entry in equation (2) and for the map period corresponding to time $k=1$. Part (a) refers to the four predictor specification of ΔT_2 ; part (b), to the three predictor specification of ΔT_2 . Part (c) refers to the verification of $\hat{\Delta T}_2$ from equation (4) applied to test time $k=2$. Part (d) refers to the verification of $\tilde{\Delta T}_2$ from equation (5) applied to time $k=2$.

	Step no.	Variable entered	Mult. Corr. Coeff., step J	F_J upon entry	Coeff. of Jth var.	% exp. var.
(a)	J=1	ΔT_1	0.7763	324.625	1.20781	60.27
	J=2	ΔZ	0.8149	38.915	0.02242	66.41
	J=3	$2\bar{T}_1$	0.8322	19.600	-0.14271	69.25
	J=4	$2\bar{T}_2$	0.8328	0.712	-0.01269	69.35
Constant Term -----					74.77295	
(b)	J=1	ΔT_1	0.7763	324.625	1.22177	60.27
	J=2	ΔZ	0.8149	38.915	0.02214	66.41
	J=3	$2\bar{T}_2$	0.8259	12.028	-0.04019	68.21
Constant Term -----					22.1258	
(c)	J=1	$\hat{\Delta T}_2$	0.6543	160.212	0.93228	42.81
(d)	J=1	$\tilde{\Delta T}_2$	0.6995	205.054	0.95789	48.93

The verification of a prediction on an independent sample-set such as that of map-time 2, is judged to be significant when a large F_1 -statistic results for either $\hat{\Delta T}_2$ or $\widetilde{\Delta T}_2$ compared to F_1^C , the critical value necessary at the 95% level (Table 1, with $J=1$). In other words, the question to be answered is whether the verifying F-statistic used upon independent test-data is greater than the critical F required for the 95% confidence level, i.e., is $F(1,216) \geq F_\alpha(1,216)$ with probability $1-\alpha \geq 0.95$? If the indicated F-statistic is sufficiently large, then there is a probability $p \geq 95\%$ of a linear relationship between ΔT_2 and the test variables (4) or (5). In parts (c) and (d) of Table 2, both F-statistics are sufficiently high to refute the probability of a chance relationship, although $\widetilde{\Delta T}_2$ (based upon equation (5)) is found to have a higher F-value than that of $\hat{\Delta T}_2$ of (4).

C. REQUIREMENTS FOR A USEFUL SPECIFICATION FOR ΔT_2

A useful specification will be defined as one satisfying the two criteria listed below.

In the first place, the specification equation (4) or (5) at each step J must be considered significant at the 95% confidence level using the F-statistic upon specification:

$$F(J,n-J-1) = \frac{\% \text{ mean sq. var. expl. by (4) or (5)}}{\% \text{ mean sq. var. unexpl. after use of (4) or (5)}} \quad (6)$$

The F-statistic ($J=1, \dots, P$) of (6) is very nearly identical to the computation of R_J^2 , where R_J is the multiple correlation coefficient at the J th step of entry in Table 2(a,b). The F-statistic of (6) is significant at a confidence level in excess of 95% whenever the F-statistic at $J=P$ exceeds the fiducial limit F :

$$F(P, n-P-1) \geq F_{\alpha}(P, n-P-1), \quad \alpha = .05 \quad (7)$$

This requirement is conservatively satisfied at the final step $J=P$ with $n=216$, whenever $R_p \geq 0.50$.

The second criterion for the test variables $\hat{\Delta T}_2$ and/or $\tilde{\Delta T}_2$ must also satisfy the inequality (7) with $P=1$, for there now exists only one way of applying the specification equation to the verification test data of time $k+1$. This latter criterion makes a requirement upon the time stability of the specification equation, a concept already used in III(A) in deciding upon the sampling procedures to be used.

The second criterion may be most conveniently judged by computing the simple correlation coefficients $R(\Delta T_2, \hat{\Delta T}_2)_{k+1}$ or $R(\Delta T_2, \tilde{\Delta T}_2)_{k+1}$, depending upon whether the four- or three-predictor regression (4) or (5) is being tested. The statistics are shown, for example in column 4 of Table 2 (c,d) as they pertain to map 2.

D. ASSESSMENT OF THE USEFULNESS OF THREE-PREDICTOR RELATIVE TO FOUR-PREDICTOR CASES

The test used in criterion 2 of III(B) was made at every verification-time $k=2, \dots, 14$ with the appropriate coefficient matrices of (4) and (5), respectively. It was found that the three-predictor equation led to the majority of stable verifications based upon consistently larger values of the test-statistics $R(\Delta T_2, \tilde{\Delta T}_2)$ compared to $R(\Delta T_2, \hat{\Delta T}_2)$. This is equivalent to saying that the three-predictor equation (5) gave a consistently higher F-level upon verification than did the four-predictor equation (4). For the reasons just cited and for economy of display, only the tabulations of specification and prediction of $\tilde{\Delta T}_2$ (the three-predictor mode) will be given in IV, which follows. Furthermore, the useful rule for a satisfactory specification, $R \geq 0.5$ will be adhered to,

at least in the sense of providing a guide line to a statistically significant prediction.

IV. STATISTICAL RESULTS AND INTERPRETATIONS

A. TABULAR LISTINGS OF THE INDIVIDUAL SPECIFICATIONS AND VERIFICATIONS

The results of the specification of ΔT_2 for map 1 and the application to the prediction of map 2 have already been listed in Table 2. Henceforth the tabular listings will be based upon the use of the three-predictor equations for both specification and verification. As an example, the results of the specification-prediction process for the case of map 2 proceeding to map 3 are listed in Table 3.

TABLE 3. (a) Specification of ΔT_2 by means of three predictors and their order of entry in equation (2) for the map corresponding to time $k=2$. (b) the predictand verification for $\widetilde{\Delta T}_2$ at time $k=3$, tested using transgenerated equation (5) with the coefficients resulting from map 2.

	Step no.	Variable entered	Mult. Corr. Coeff., step J	F_J upon entry	Coeff. of Jth var. after J=3	% exp. var.
(a)	J=1	ΔT_1	0.6480	154.920	1.25588	41.99
	J=2	ΔZ	0.7051	32.748	0.01502	49.72
	J=3	$2\bar{T}_2$	0.7140	5.466	-0.03471	50.99
	Constant Term -----				18.67230	
(b)	J=1	$\widetilde{\Delta T}_2$	0.6049	123.476	1.01990	36.59
	Constant Term -----				0.54359	

TABLE 4. (a) Specification of ΔT_2 by means of three predictors and their order of entry in equation (2) for the map corresponding to time $k=3$. (b) The predictand verification for $\widetilde{\Delta T}_2$ at time $k=4$, tested using the transgenerated equation (5) with the coefficients resulting from map 3.

	Step no.	Variable entered	Mult. Corr. Coeff., step J	F_J upon entry	Coeff. of Jth var. after J=3	% exp. var.
(a)	J=1	ΔT_1	0.5846	111.1034	1.30967	34.17
	J=2	ΔZ	0.6514	30.5582	0.01701	42.43
	J=3	\bar{T}_2	0.6626	5.5326	0.03524	43.90
Constant Term -----					-19.08235	
(b)	J=1	$\widetilde{\Delta T}_2$	0.6664	170.9637	1.18358	44.41
	Constant Term -----					-0.11233

TABLE 5. (a) Specification of ΔT_2 by means of three predictors and their order of entry in equation (2) for the map corresponding to time $k=4$. (b) The predictand verification for $\widetilde{\Delta T}_2$ at time $k=5$, tested using the transgenerated equation (5) with the coefficients resulting from map 4.

	Step no.	Variable entered	Mult. Corr. Coeff., Step J	F_J upon entry	Coeff. of Jth var. after J=3	% exp. var.
(a)	J=1	ΔT_1	0.6423	150.3109	1.63211	41.26
	J=2	ΔZ	0.7037	34.8372	0.03241	44.25
	J=3	\bar{T}_2	0.7151	7.0636	-0.04216	51.14
Constant Term -----					23.47249	
(b)	J=1	$\widetilde{\Delta T}_2$	0.5810	109.0053	0.83761	33.76
	Constant Term -----					-0.22636

TABLE 6. (a) Specification of ΔT_2 by means of three predictors and their order of entry in equation (2) for the map corresponding to time k=5. (b) The predictand verification for ΔT_2 at time k=6, tested using the transgenerated equation (5) with the coefficients resulting from map 5.

	Step no.	Variable entered	Mult. Corr. Coeff., step J	F_J upon entry	Coeff. of Jth var. after J=3	% exp. var.
(a)	J=1	ΔT_1	0.4798	64.0106	1.28656	23.02
	J=2	ΔZ	0.6168	51.6145	0.04833	38.04
	J=3	\bar{T}_2	0.6175	0.3010	-0.00859	38.13
Constant Term -----					4.17122	
(b)	J=1	$\widetilde{\Delta T}_2$	0.5753	105.8482	0.72407	33.09
	Constant Term -----					0.14901

TABLE 7. (a) Specification of ΔT_2 by means of three predictors and their order of entry in equation (2) for the map corresponding to time k=6. (b) The predictand verification for ΔT_2 at time k=7, tested using the transgenerated equation (5) with the coefficients resulting from map 6.

	Step no.	Variable entered	Mult. Corr. Coeff., Step J	F_J upon entry	Coeff. of Jth Var. after J=3	% exp. var.
(a)	J=1	ΔT_1	0.5615	98.5142	0.97251	31.52
	J=2	\bar{T}_2	0.6417	34.9574	-0.06165	41.18
	J=3	ΔZ	0.6666	12.4533	0.01840	44.44
Constant Term -----					33.53210	
(b)	J=1	$\widetilde{\Delta T}_2$	0.4619	58.0505	0.87025	21.34
	Constant Term -----					0.71712

TABLE 8. (a) Specification of ΔT_2 by means of three predictors and their order of entry in equation (2) for the map corresponding to time k=7. (b) The predictand verification for $\hat{\Delta T}_2$ at time k=8, tested using the transgenerated equation (5) with the coefficients resulting from map 7.

	Step no.	Variable entered	Mult. Corr. Coeff., step J	F_J upon entry	Coeff. of Jth var. after J=3	% exp. var.
(a)	J=1	ΔT_1	0.4481	53.7527	0.95690	20.08
	J=2	ΔZ	0.5919	49.0300	0.05084	35.03
	J=3	\bar{T}_2	0.6090	6.9456	0.04418	37.09
Constant Term -----					-23.46455	
(b)	J=1	$\tilde{\Delta T}_2$	0.6588	164.0839	1.24020	43.40
	Constant Term -----					-2.38063

TABLE 9. (a) Specification of $\Delta \bar{T}_2$ by means of three predictors and their order of entry in equation (2) for the map corresponding to time k=8. (b) The predictand verification for $\hat{\Delta \bar{T}}_2$ at time k=9, tested using the transgenerated equation (5) with the coefficients resulting from map 8.

	Step no.	Variable entered	Mult. Corr. Coeff. step J	F_J upon entry	Coeff. of Jth var. after J=3	% exp. var.
(a)	J=1	ΔT_1	0.5594	97.4484	1.26707	31.29
	J=2	ΔZ	0.6643	48.9321	0.05761	44.12
	J=3	\bar{T}_2	0.6666	1.2026	0.02007	44.44
Constant Term -----					-12.24481	
(b)	J=1	$\tilde{\Delta \bar{T}}_2$	0.5439	89.9256	0.43759	29.59
	Constant Term -----					0.75761

TABLE 10. (a) Specification of ΔT_2 by means of three predictors and their order of entry in equation (2) for the map corresponding to time k=9. (b) The predictand verification for $\hat{\Delta T}_2$ at time k=10, tested using the transgenerated equation (5) with the coefficients resulting from map 9.

	Step no.	Variable entered	Mult. Corr. Coeff., step J	F_J upon entry	Coeff. of Jth var. after J=3	% exp. var.
(a)	J=1	ΔZ	0.3859	37.4493	0.02426	14.89
	J=2	ΔT_1	0.5368	41.6514	0.69409	28.81
	J=3	\bar{T}_2	0.5785	14.8342	0.06375	33.47
Constant Term -----					-34.89899	
(b)	J=1	$\widetilde{\Delta T}_2$	0.1449	4.5912	-0.17341	2.10
	Constant Term -----					1.31401

TABLE 11. (a) Specification of ΔT_2 by means of three predictors and their order of entry in equation (2) for the map corresponding to time k=10. (b) The predicted verification for $\hat{\Delta T}_2$ at time k=11, tested using the transgenerated equation (5) with the coefficients resulting from map 10.

	Step no.	Variable entered	Mult. Corr. Coeff., step J	F_J upon entry	Coeff. of Jth var. after J=3	% exp. var.
(a)	J=1	\bar{T}_2	0.3431	28.5494	-0.09331	11.77
	J=2	ΔT_1	0.3480	0.8302	0.06180	12.11
	J=3	ΔZ	0.3506	0.4407	0.00469	12.30
Constant Term -----					52.30643	
(b)	J=1	$\widetilde{\Delta T}_2$	0.1015	2.2278	-0.10086	1.03
	Constant Term -----					1.17698

TABLE 12. (a) Specification of ΔT_2 by means of three predictors and their order of entry in equation (2) for the map corresponding to time $k=11$. (b) The predictand verification for $\widetilde{\Delta T}_2$ at time $k=12$, tested using the transgenerated equation (5) with the coefficients resulting from map 11.

	Step no.	Variable entered	Mult. Corr. Coeff., step J	F_J upon entry	Coeff. of Jth var. after J=3	% exp. var.
(a)	J=1	ΔT_1	0.4562	56.2325	0.96817	20.81
	J=2	\bar{T}_2	0.5057	13.6216	-0.08226	25.57
	J=3	ΔZ	0.5298	7.3782	0.02377	28.07
	Constant Term -----					43.16838
(b)	J=1	$\widetilde{\Delta T}_2$	0.5698	102.8863	1.14851	32.47
	Constant Term -----					4.59990

TABLE 13. (a) Specification of ΔT_2 by means of three predictors and their order of entry in equation (2) for the map corresponding to time $k=12$. (b) The predictand verification for $\widetilde{\Delta T}_2$ at time $k=13$, tested using the transgenerated equation (5) with the coefficients resulting from map 12.

	Step no.	Variable entered	Mult. Corr. Coeff., step J	F_J upon entry	Coeff. of Jth var. after J=3	% exp. var.
(a)	J=1	ΔT_1	0.6457	153.0436	1.57667	41.70
	J=2	ΔZ	0.7031	32.6091	0.02136	49.44
	J=3	\bar{T}_2	0.7114	5.0147	0.04039	50.61
	Constant Term -----					-20.36539
(b)	J=1	$\widetilde{\Delta T}_2$	0.6688	173.2133	0.76579	44.73
	Constant Term -----					-1.61974

TABLE 14. (a) Specification of ΔT_2 by means of three predictors and their order of entry in equation (2) for the map corresponding to time k=13. (b) The predictand verification for ΔT_2 at time k=14, tested using the transgenerated equation (5) with the coefficients resulting from map 13.

	Step no.	Variable entered	Mult. Corr. Coeff., step J	F_J upon entry	Coeff. of Jth var. after J=3	% exp. var.
(a)	J=1	ΔT_1	0.5876	112.8828	1.00762	34.53
	J=2	ΔZ	0.7372	92.4117	0.04857	54.34
	J=3	\bar{T}_2	0.7399	1.9182	0.02137	54.75
Constant Term -----					-11.92155	
(b)	J=1	$\widetilde{\Delta T}_2$	0.6030	122.2797	1.01096	36.36
	Constant Term -----					1.40262

TABLE 15. (a) Specification of ΔT_2 by means of three predictors and their order of entry in equation (2) for the map corresponding to time k=14. (b) The predictand verification for ΔT_2 at time k=1, tested using the transgenerated equation (5) with the coefficients resulting from map 14.

	Step no.	Variable entered	Mult. Corr. Coeff., step J	F_J upon entry	Coeff. of Jth var. after J=3	% exp. var.
(a)	J=1	ΔT_1	0.5100	75.2309	1.12036	26.01
	J=2	ΔZ	0.5982	32.4248	0.03983	35.79
	J=3	\bar{T}_2	0.6485	22.9468	0.09734	42.06
Constant Term -----					-52.64392	
(b)	J=1	$\widetilde{\Delta T}_2$	0.7011	206.8751	0.72137	49.15
	Constant Term -----					-0.57721

In addition it is desirable to list all corresponding sets of ΔT_2 specification and verification for each of the twelve subsequent pairs of days. For example, Table 4 is analogous to Table 3, except that the initial specification is for time $k=3$ and the verification using the transgenerated equation is then applied to $k=4$. The remaining Tables 5-15 are listed in sequence in view of a similarity in the pattern of the statistics presented in the listings, when useful specification-predictions occur. In contrast, a distinct change in this pattern occurs when a specification-prediction fails, an example of which occurs at map-time $k=10$.

In order to exploit the data for maximum usefulness, the specification from $k=14$ was used as a predictor for $k=1$, the results of which are shown in Table 15.

B. A SUMMARY OF THE MEAN SPECIFICATION-PREDICTION RESULTS

A statistical parameter that clearly summarizes the specification-verification results for the two-map statistical sequences is the final percentage explained variance. Hence it is advantageous to list this statistic for each specification map together with its corresponding verification. This is done in Table 16.

The parameter $\overline{R^2}$ is identified with the mean overall explained variances in the set of twelve useful specifications and corresponding verifications, which appear at the end of columns 2 and 7. Then \overline{R} , the mean coefficient of determination, has the value $\overline{R} = 0.6911$ and $.6082$ at the indicated stages, respectively.

Table 16 also lists in column 3, for each specification map k , the percentage unexplained variance, which is given by $(1-R^2)$.

TABLE 16. Summary of percentage explained variances of ΔT_2 at the specification step k, and at step (k+1) in the verification process.

Map-time k	% Exp. Var. ΔT_2 on map k	% Unexp. Var. for map k	Standard Deviation	Standard Error	Map-time k+1	% Exp. Var. ΔT_2 on map k+1
1	68.21	31.79	5.30951	2.9736	2	48.93
2	50.59	49.41	5.20436	3.6400	3	36.59
3	43.90	56.10	5.43297	3.9325	4	44.41
4	51.14	48.86	6.40811	4.4229	5	33.76
5	38.13	61.87	5.82407	4.5978	6	33.09
6	44.44	55.56	4.83820	3.5816	7	21.34
7	37.09	62.91	5.89500	4.6610	8	43.40
8	44.44	55.56	6.62934	4.3862	9	29.59
9	33.47	66.53	5.75243	4.1150	10	2.10
10	12.30	87.70	5.14620	4.8410	11	10.92
11	28.07	71.93	5.15380	4.2230	12	32.47
12	50.16	49.84	5.65208	4.0115	13	44.73
13	54.75	45.25	5.12623	3.4371	14	36.36
14	42.06	57.94	6.32972	4.8106	1	49.15
Mean:	45.11	54.89	5.6710	4.2171		36.99

In addition, the table lists the standard deviation σ of ΔT_2 and its standard error ($\sigma_{Y/X}$) for each time $k=1, \dots, 14$. The standard errors in each case may be computed from equation (8):

$$\frac{\sigma_{Y/X}^2}{\sigma^2} = \left(\frac{\text{standard error}}{\text{standard deviation}} \right)^2 = 1-R^2 \quad (8)$$

It should be noted that the two "unreliable" prediction cases (10 and 11), which occur because of a single anomalous specification at $k=10$, have not been included for averaging purposes in Table 16.

C. NORMAL PATTERNS OF PREDICTOR-ENTRY FOR USEFUL SPECIFICATIONS OF ΔT_2

The statistical feature most apparent among the useful ($R \geq 0.5$) specification cases listed in Tables 2 through 15 was the order of entry of the predictors. When the multiple correlation coefficient had values in excess of entry of 0.6, the order of entry in these tables was consistently ΔT_1 , ΔZ , and \bar{T}_2 . As mentioned in IIIA, it is the value of the F-statistic upon entry which determines the order of entry, and in ten of the twelve cases considered to be useful, the predictors entered in this particular order. The other two cases of useful specification corresponded to the data samples for maps 6 and 11, in both of which the order of entry was ΔT_1 , \bar{T}_2 , and ΔZ . For both of these cases the explained variance for specification was acceptable due to the large F upon entry at the first step, i.e., that which introduced the variable ΔT_1 .

An "unreliable" assessment was given to the specification equation for map 9 (Table 10) for which the irregular order of entry (ΔZ , ΔT_1 , \bar{T}_2) and associated relatively small F upon entry values led to coefficients

which could not be meshed with those entering the specification equation for map 10. Thus map 10 gave poor verification of map 9, and also poor specification when introduced for the verification of map 11. The instability of these two map-sets may be seen at once by reviewing Tables 10 and 11, with particular attention given to the coefficient matrix of the variables ΔT_1 , ΔZ , \bar{T}_2 . Note particularly the systematic change in the matrices shown relative to those entered immediately before and after maps 9 and 10.

Using percentage explained variance as a guide to the verification of maps 10 and 11, it is apparent from Table 16 that the map-sequence 10-11 should be deleted as useful specification-prediction combinations. When this has been done, the mean fractional explained variance upon specification and verification are obtained: 0.4511 and 0.3699, respectively. These means are above the tolerance of acceptable fractional explained variance at both specification and verification, namely 0.25.

At this point a brief discussion of the option of selecting \bar{T}_2 rather than \bar{T}_1 and \bar{T}_2 is applicable. The primary reason for this decision was the high value of the linear correlation coefficient, $r(\bar{T}_2, \bar{T}_1)$, in all useful specifications. As an example, the correlation matrix based upon map time 2 is shown in Table 17 below.

TABLE 17. The predictand-predictor linear correlation matrix for map 2.

	ΔT_2	ΔT_1	ΔZ	\bar{T}_2	\bar{T}_1
ΔT_2	1.000	.648	.124	.141	.041
ΔT_1	.648	1.000	-.227	.363	.230
ΔZ	.124	-.227	1.000	-.048	-.266
\bar{T}_2	.141	.363	-.048	1.000	.768
\bar{T}_1	.041	.230	-.286	.768	1.000

Note in particular that $\bar{r}(\bar{T}_1, \bar{T}_2) = 0.768$ so that there exists considerable redundancy of similar information when both \bar{T}_1 and \bar{T}_2 are retained in a four-variable specification. The decision to eliminate \bar{T}_1 rather than \bar{T}_2 by the control-delete option of BMD02R is then based upon the small standard deviation of the observed \bar{T}_1 , relative to that of \bar{T}_2 (approximately in the ratio of 1 to 3). Furthermore, using the CONDEL option in testing the three predictor equation, which included \bar{T}_1 rather than the deleted \bar{T}_2 , resulted in a slight shrinkage of the multiple correlation coefficients upon verification.

V. EXTENSION OF THE RESULTS TO 24-HOUR SPECIFICATIONS

A. RE-EXAMINATION OF THE FIVE-DAY SPECIFICATION PROCEDURE FOR POSSIBLE EXTENSION

In the preceding discussion, ΔT_2 values centered at the five-day mean map time k were found to be linearly related to the independent variables ΔT_1 , ΔZ and \bar{T}_2 by means of a statistical equation of the following form:

$$\Delta T_2 = B_0 + B_1 \Delta T_1 + B_2 \Delta Z + B_3 \bar{T}_2 \quad (9)$$

where each of the variables of the right side is likewise time-centered at map time k . In addition, the order of importance of the variables on the right side of (9), in thirteen of the fourteen cases, was significant using the step-wise regression of the BMD02R program. The order was consistently ΔT_1 , ΔZ , \bar{T}_2 .

In order to further establish the stability of (9), a verification test was conducted, based upon the results at time k , to the five-day mean data at time $k+1$. This resulted in only a slight shrinkage in percentage explained variance using the same coefficient matrix (B_0, B_1, B_2, B_3) on the independent data of map $k+1$.

This stability test was desirable to assess the usefulness of the diagnostic equation (9) in deriving a valid specification. In the process of testing (9) for statistical stability, unreliable specification in one case, $k=10$, led to two cases of inadequate verification, at times $k=10$ and 11 . Statistically this has been explained in IV as due to lack of homogeneity in the five-day mean coefficients B_0, B_1, B_2, B_3 , which occurred at map-time $k=10$, relative to the longer-term sample means of these coefficients over the full test-period of 14 maps.

A pertinent conclusion to be drawn, then, is that the statistical model evolved in IV is useful in obtaining a valid specification for the effective cloud-top level change for a five-day mean cloud state at grid points (i,j), using the Standard Atmosphere lapse rate of $6.5\text{K}(\text{km})^{-1}$. Thus a negative change in ΔT_2 of 6.5K is equivalent to an effective cloud top ascent of 1 kilometer, if fully overcast conditions exist.

On the other hand, if the mean cloud cover at an oceanic grid point remains constant at \bar{C} , where $\bar{C} < 1.0$, and an observed decrease in T_2 occurs, then the ascent in the effective cloud tops (which covers only the fractional area \bar{C}) is deductible from

$$\Delta Z_{\text{Top}} = - \frac{\Delta T_2}{\gamma \cdot \bar{C}}, \quad \gamma = 6.5 \text{ K/km}$$

This formula follows since the window channel radiometer senses the relatively constant ocean surface temperature in cloud-free areas, and the effective cloud top level over the fractional area \bar{C} of cloud-cover.

Finally, the parameters ΔT_1 , ΔZ and \bar{T}_2 appear to provide the necessary spatial and temporal stability to employ the specification scheme over time spans extending as long as ten days in most of the cases listed (Tables 2,...,15).

B. 24-HOUR STATISTICAL SPECIFICATION OF ΔT_2 AND THE PHYSICAL INTERPRETATION OF THE PREDICTOR VARIABLES

The problem to be considered now is that of the analogous use of strictly 24 hourly data. It would be possible to use the BMD02R program to obtain a diagnostic equation of the form:

$$\Delta T_2(24) = C_0 + C_1 \Delta T_1 + C_2 \Delta Z + C_3 \bar{T}_2 \quad (10)$$

based entirely upon independent variables observed at 24 hourly intervals,

and time-centered twelve hours before the latest data report has been received. The assumption is that good daily mapped versions of the T_2 and T_1 fields have been received in suitably calibrated digitized T_{BB} form from the designated processor in Washington (NESS), and communicated instantly to the satellite data-user in the field.

The tests applied in this paper do not include 24-hour best-fit specification because ΔT_2 , ΔT_1 , ΔZ and T_2 were not available in synoptically time-centered form at appropriate times. However, if useful specifications were derived on the basis of five-day averaged data of the same form, it is expected that the specification equations of at least the same or better efficiency should result for 24-hour averaged data. This concept will be discussed from the point of view that ΔT_2 depends upon basic atmospheric physical parameters, which are reflected through ΔT_1 , ΔZ and T_2 as derived products. Moreover, the time-sequencing of the physical relationships, and therefore of the specifications, should be more precise for shorter periods (24 hours) than for longer period specifications, such as five-day periods. During this longer period, atmospheric diffusion tends to smear the effects of the physical relationships which bear on ΔT_2 .

Equation (10) is therefore proposed as a significant regression to be applied to 24-hour mean data fields much as such regressions were found to be descriptive for five-day means. Further supporting arguments below are for a 24-hour specification equation of form (10) based upon the physical usefulness of the variables on the right side of (10).

1. The 24-Hour Time Change, ΔT_1

Raschke and Bandeen (1967) have shown that properly calibrated values of T_1 (when used in conjunction with T_2) yield the mean relative

humidity in the tropospheric layer extending between six to ten kilometers. ΔT_1 may therefore be interpreted as either a change in the mean relative humidity of this column or as a vertical velocity producing the same humidity effect.

Beran, et al. (1968) showed that 24-hour positive changes in ΔT_1 are associated with areas of convergence near the 200 mb jet level, with resultant downward forced vertical motion giving reduced mean humidities in the upper convergent tropospheric layer. The use of five-day means in the present investigation, as contrasted with that of Beran, resulted in the loss of some discrimination regarding ΔT_1 , since the five-day mean fields of ΔT_1 , near the mean polar front jet had much smaller gradients than were found by Beran et al. on a single-day change basis.

2. The 24-Hour Height Change at 500 mb, ΔZ

24-hour height change fields at 500 mb are employed here since they have been found to be useful in analysis of cloud-development seen in satellite pictures. In that context, Z is usually presented in its scale-pattern decomposition:

$$\begin{aligned} Z &= Z_{SR} + Z_{SD} \\ \Delta Z &= \Delta Z_{SR} + \Delta Z_{SD} \end{aligned} \tag{11}$$

Here, since the long-wave field Z_{SR} is temporally conservative, it follows that $\Delta Z = \Delta Z_{SD}$, and therefore,

$$\Delta Z = Z_{SD}(t=0) - Z_{SD}(t=-24).$$

Distributions of ΔZ_{SD} are known to manifest the short wave 500-mb vorticity patterns which are superimposed upon the large-scale steering patterns, the latter being the Z_{SR} fields at 500 mb. In turn, the ΔZ_{SD}

patterns are related to photographic features of cloud analysis, e.g., the comma-shaped cloud with maxima of positive vorticity advection. Thus ΔZ patterns occurring over the preceding 24 hours represent changes in the relative vorticity patterns over the area and are instrumental not only in effecting changes in the photographic depiction of cloud masses or bands but also changes in their vertical extent, reflected by parameter T_2 . In summary, the parameter ΔZ , as defined for the past 24 hours, should be expressive of a cloud-structure change in ΔT_2 resulting from the vorticity-advection change field within the grid area.

3. The Large-Scale Steering Parameter, T_2

Finally, in scale decomposition applications, the 500-mb SR field is known to represent the steering component of the 500-mb wind field insofar as vorticity changes are concerned. Space-average contour height fields equivalent to the Z_{SR} field were not available, however, for any of the tests conducted in this study. Nevertheless, a time-smoothed 500-mb map is very nearly equivalent in its long-wave steering characteristic to the space-smoothed Z_{SR} -maps which may be derived from an individual 500-mb map, at the time-centered date.

The Northern Hemisphere five-day mean contour heights have been added to the data file for use in a BMD02R program for the same set of 15 data periods as were originally investigated. This was done in a manner exactly analogous to that used in forming fields of \bar{T}_2 , which is a predictand entering the right side of (9). The five-day Northern Hemisphere fields of \bar{T}_2 , for the 1966 period of NIMBUS II, have been intensively studied by Professor F. L. Martin, who has found that they afford a striking resemblance to the corresponding five-day mean 500-mb contour fields, period-for-period north of 15° latitude.

This fact suggested the supplementary test of correlating the five-day means of \bar{T}_2 and \bar{Z} over the test area of this investigation (216 grid points), based upon a pooled series of five consecutive maps of five-day means of both \bar{T}_2 and \bar{Z} . The ensuing regression analysis gave the result:

$$\bar{Z}(\text{gpm}) = 1919.0293 + 6.9477\bar{T}_2$$

with a linear correlation: $R(\bar{Z}, \bar{T}_2) = .8506$.

This result gives a rationale for employing \bar{T}_2 in the correlation originally tested in the specification equation (9) where, except for ΔZ , only radiometric variables were entered into the regression equation. It thus becomes clear that the five-day mean \bar{T}_2 field has nearly the same smoothed properties as the five-day mean \bar{Z} -field.

It is proposed that, for the 24-hour specification, the use of the time-centered field of T_2 , when space-smoothed to grid points on an NMC synoptic-scale chart, reflects primarily the SR-advecting component of the 500 mb field. Thus in (10), the space-smoothed T_2 field should by analogy perform the role of the 500-mb SR field in steering the individual disturbances. For this reason the space-smoothed T_2 (from the 12-hour earlier swath) has been included as predictor in the 24-hour specification equation (10) for ΔT_2 .

Finally, it has been concluded, using both the references and tests cited here, including related knowledge from satellite-picture interpretations, that the three parameters ΔT_1 , ΔZ , and T_2 which appear in (10), are likely to be descriptive of ΔT_2 . It is recommended that a test be made of this hypothesis using the 24-hour specification procedure.

From the preceding discussion, each of the parameters just cited is representative of a large-scale dynamical factor affecting cloud-structure

in the atmosphere. While there is undoubtedly non-linear interaction between the physical parameters proposed, the use of a linear regression model tends to separate nonlinear effects into linearized ones. Hence the following summary of the statistical parameters included in (10) is presented here with the suggested physical interpretation which they represent:

- (1) ΔT_1 is indicative of vertical motion change over the past 24 hours.
- (2) ΔZ is indicative of the relative vorticity propagation by steering and of development during the steering.
- (3) The space-smoothed field T_2 is indicative of the space-smoothed 500-mb field. It is also indicative of a 24-hour mean radiometric estimate of the cloud-top level over oceanic grid points. In this later connection, $T_2(i,j)$ should also be related to average surplus (deficit) of radiative energy in the mean column at (i,j) and therefore to the eddy-generation effect on an existing or incipient disturbance (Katayama, 1967).

VI. PROPOSALS FOR FUTURE STUDY; A SUMMARY

In order for an equation of form (10) to have predictive value for a period of 12 hours over a given test area, it will be necessary to have a polar-orbiting satellite such as NIMBUS IV, reporting T_1 and T_2 data in equivalent blackbody form at 12 hourly intervals. In this way, the 24-hour interval centered 12-hours before receipt of the latest report would provide the resulting specification equation, and could then be applied to a time period centered now at time $t=0$, concurrent with receipt of the latest radiometric maps provided ΔT_1 can be computed.

This scheme would require the $t=0$ field of T_2 , smoothed to synoptic scale, as well as prognosticated fields of ΔT_1 and ΔZ for the succeeding twelve hours. A 24-hour ΔZ prognosis is presently available from the Primitive Equation model. Prognostic fields of ΔT_1 are not presently available; however it is not unreasonable to suggest that with further tests and evaluation using satellite-provided water-vapor channel fields such a prognostic scheme could be developed.

NIMBUS IV included a temperature-humidity infrared radiometer (THIR) experiment, the purpose of which was to measure by channels 1 and 2 daytime and nighttime surface and cloud-top temperatures and cloud mapping; by channel 1, atmospheric water vapor mapping (NIMBUS IV User's Guide, 1970). THIR data are archived in separate daytime and nighttime swaths. The problem is then one of obtaining prognosticated 12-hour fields of T_1 , so that $T_1(12) - T_1(-12) = \Delta T$ is known for use in (10).

If the temperature distribution is initially known, the vertical distribution as well as total amount of water vapor in a vertical column above 500 mb may be inferred (Raschke and Bandeen, 1967). The inference

of water-vapor absorber mass below 500 mb has not been very successful for radiances in the 6.7μ channel because the effective-intensity emission in channel 1 arises from a level in the upper troposphere (Shenk and Salomonson, 1970). Furthermore, characteristic T_1 configurations provide information about the upper-tropospheric wind field. Martin and Salomonson (1970) have used radiometric information from NIMBUS II MRIR to locate the core of the subtropical jet and deduce maximum wind speed.

Thus since T_2 is indicative of in-cloud temperature and is subject to change with changing cloud-structure much as a satellite photograph indicates, the most favorable radiometric field to consider for prognostication is that of T_1 . A successful prediction in the T_1 field is reasonable to hypothesize since T_1 is descriptive of the mean water-vapor mass above 500 mb; that is, at a level generally above the top of the middle-clouds. With this prognosticated T_1 -field, a field of ΔT_1 would become available for use with the known prognostic field of ΔZ , and the current T_2 field. Thus ΔT_2 , the most variable radiometric parameter of equation (10), would be amenable to computation by the regression method proposed here.

This avenue of approach seems to offer a fruitful use of MRIR radiances as predictors of effective cloud-top change. Furthermore, the result would afford a three-dimensional aspect to cloud-distribution forecasting.

BIBLIOGRAPHY

1. Beran, D. W., E. S. Merritt and D. T. Chang, Interpretation of Baroclinic Systems and Wind Fields as Observed by NIMBUS II MRIR, Final Report, Contract NAS 5-10334, Allied Research Associates, Concord, Mass., 1968.
2. Dixon, W. J., Biomedical Computer Programs, Health Sciences Computing Facility, University of California at Los Angeles, 1966.
3. Katayama, A., "On the Radiation Budget of the Troposphere over the Northern Hemisphere (III)", Journal of the Meteorological Society of Japan, Vol. 45, No. 1, February 1967.
4. Martin, Frank L., and Vincent V. Salomonson, "Statistical Characteristics of Subtropical Jet-Stream Features in Terms of MRIR Observations from NIMBUS II", Journal of Applied Meteorology, Vol. 9, No. 3, June 1970.
5. Miller, R. G., "Statistical Predictions by Discriminant Analysis", Meteorological Monographs, 4, No. 25, 1962.
6. NIMBUS Project, 1966: NIMBUS II User's Guide, NASA, Goddard Space Flight Center, Greenbelt, Maryland.
7. NIMBUS Project, 1970: NIMBUS IV User's Guide, NASA, Goddard Space Flight Center, Greenbelt, Maryland.
8. Raschke, Ehrhard, and William R. Bandeen, "A Quasi-Global Analysis of Tropospheric Water Vapor Content from TIROS IV Radiation data", Journal of Applied Meteorology, Vol. 6, June 1967.
9. Shenk, W. E., and V. V. Salomonson, "Visible and Infrared Imagery from Meteorological Satellites", Applied Optics, Vol. 9, No. 8, August 1970.

INITIAL DISTRIBUTION LIST

	No. Copies
1. Defense Documentation Center Cameron Station Alexandria, Virginia 22314	2
2. Library, Code 0212 Naval Postgraduate School Monterey, California 93940	2
3. Department of Meteorology, Code 51 Naval Postgraduate School Monterey, California 93940	3
4. Professor Frank L. Martin Department of Meteorology Naval Postgraduate School Monterey, California 93940	6
5. LCDR P. B. Knostman, USN 292 Monrovia Avenue Long Beach, California 90803	1
6. Assoc. Professor Wm. van der Bijl Department of Meteorology Naval Postgraduate School Monterey, California 93940	1

DOCUMENT CONTROL DATA - R & D

(Security classification of title, body of abstract and indexing annotation must be entered when the overall report is classified)

1 ORIGINATING ACTIVITY (Corporate author) Naval Postgraduate School Monterey, California 93940		2a. REPORT SECURITY CLASSIFICATION Unclassified	
		2b. GROUP	
3 REPORT TITLE Statistical Results Concerning the Radiometric Temperature Changes Sensed by NIMBUS II MRIR in the Vicinity of the Subtropical Jet			
4 DESCRIPTIVE NOTES (Type of report and, inclusive dates) Master's Thesis; September 1971			
5 AUTHOR(S) (First name, middle initial, last name) Paul Brayton Knostman			
6 REPORT DATE September 1971		7a. TOTAL NO. OF PAGES 47	7b. NO. OF REFS 9
8a. CONTRACT OR GRANT NO.		9a. ORIGINATOR'S REPORT NUMBER(S)	
b. PROJECT NO.			
c.		9b. OTHER REPORT NO(S) (Any other numbers that may be assigned this report)	
d.			
10 DISTRIBUTION STATEMENT Approved for public release; distribution unlimited.			
11. SUPPLEMENTARY NOTES		12. SPONSORING MILITARY ACTIVITY Naval Postgraduate School Monterey, California 93940	
13. ABSTRACT Radiances obtained from the 11- μ window channel by MRIR scanning radiometer of NIMBUS II were investigated in order to determine areas of time change of T_2 , which may be related to effective cloud top level of the five-day mean cloud state. A statistical model was developed that is useful in obtaining a valid specification for effective cloud top change, using a stepwise regression program. The parameters ΔT_1 , ΔZ , and \bar{T}_2 appear to provide the necessary spatial and temporal stability to employ the specification scheme over a time span of ten days. These three parameters are all highly descriptive of ΔT_2 in terms of basic atmospheric dynamical relationships. It is recommended that a test be made of this hypothesis using a 24-hour specification procedure.			

BINDERY

Thesis
K68
c.1

131317

Knostman

Statistical results
concerning the radio-
metric temperature
changes sensed by
NIMBUS II MRIR in the
vicinity of the sub-
tropical jet.

ts

Thesis
K68
c.1

131317

Knostman

Statistical results
concerning the radio-
metric temperature
changes sensed by
NIMBUS II MRIR in the
vicinity of the sub-
tropical jet.

thesK68

Statistical results concerning the radio



3 2768 002 10691 6
DUDLEY KNOX LIBRARY